


Quantum thermometry based on a cavity-QED setup

Dong Xie ^{1,*} Feng-Xiao Sun,^{2,3} and Chunling Xu¹

¹College of Science, Guilin University of Aerospace Technology, Guilin, Guangxi 541004, People's Republic of China

²State Key Laboratory of Mesoscopic Physics, School of Physics, Peking University, Beijing 100871, People's Republic of China

³Frontiers Science Center for Nano-optoelectronics & Collaborative Innovation Center of Quantum Matter, Peking University, Beijing 100871, People's Republic of China



(Received 21 April 2020; accepted 8 June 2020; published 30 June 2020)

We present a quantum thermometry scheme based on a cavity-QED setup, which attains a sensitivity with Heisenberg scaling. A stream of identical two-level systems passes through a thermal bath to be tested. Each system partially thermalizes, carrying information on the temperature of the thermal bath, and it then interacts with a dissipative single-mode cavity. The Heisenberg scaling is attained from the initial coherence of each system. The systems cannot be fully thermalized by the thermal bath. The optimal interaction time between the system and the thermal bath is derived. Direct photon detection is proved to be an optimal measurement when there is no extra thermal bath in the cavity. In the case where there is an extra thermal bath in the cavity independent of the thermal bath to be tested, homodyne detection is the optimal measurement. Moreover, we show that direct photon detection obtains less information in the case where the extra thermal bath in the cavity is in thermal equilibrium with the thermal bath. However, the optimal measurement can utilize the information from the extra thermal bath to improve the estimation precision of the temperature.

DOI: [10.1103/PhysRevA.101.063844](https://doi.org/10.1103/PhysRevA.101.063844)

I. INTRODUCTION

Quantum metrology plays a crucial role in the development of basic science and technology [1–6]. In particular, improving the precision of temperature metrology is becoming more and more important. There is a growing interest in obtaining accurate temperature measurements [7–13]. In classical physics, the best metrology precision, known as the quantum shot-noise limit (SNL), scales as $1/\sqrt{N}$, with N being the number of resources employed in the measurements. Quantum effects can help us to beat the SNL, such as squeezing [14–18] and entanglement [19,20].

Although quantum effects can improve the measurement accuracy, they are actually quite fragile. The main reason is the inevitable environmental decoherence. A realistic physical system inevitably interacts with the surrounding environment, leading to a loss in the coherence and entanglement. For a unitary parameter, such as phase and frequency, one can place the probe system in a cryogenic environment to reduce the decoherence. However, for a nonunitary parameter (temperature), the probe system must make contact with the thermal bath to obtain temperature information. Hence, decoherence is difficult to suppress. Correa *et al.* [21] investigated the fundamental limitations on temperature estimation with an individual quantum probe and found that initial coherence may not be directly linked to the overall maximization of the precision. Thomas [22] demonstrated that thermometry may be mapped onto the problem of phase estimation to obtain Heisenberg scaling. However, there are some constraints which are difficult to relax.

In a recent experiment, Kim *et al.* [23] implemented the cavity-QED scheme where a series of two-level atoms randomly passes through a single-mode cavity and showed the single-atom superradiance effect [24,25] by the initial atomical coherence. It means that the steady-state average photon number of the cavity is proportional to the square of the number of the effective coupling atoms. Cheng *et al.* [26] further showed that the Heisenberg scaling for the unitary parameter (the atom-cavity coupling strength) can be obtained with the assistance of superradiance. The advantage of the scheme is that the preparation (maintaining) of the atomic entanglement before (after) they interact with the cavity field is not required.

In this article, without preparing atomic entanglement in advance, we want to obtain the Heisenberg scaling in estimating the nonunitary parameter (temperature) with the assistance of superradiance. We propose a quantum thermometry scheme based on the cavity-QED setup. A series of injected two-level systems (TLSs) passes through the thermal bath to be tested. Then they pass through a single-mode cavity one by one. Our results show that the Heisenberg scaling for the temperature of the thermal bath can be obtained. And the initial coherence of each system and partly thermalization are necessary. The optimal thermalized time has been derived. What is more, direct photon detection is proved to be an optimal measurement when there is no extra thermal bath in the cavity. In case there is an extra thermal bath in the cavity independent of the thermal bath to be tested, homodyne detection is the optimal measurement. Moreover, we show that direct photon detection obtains less information if the extra thermal bath in the cavity is in thermal equilibrium with the thermal bath. By using the Fisher information, we find that the optimal measurement can utilize the information from the

*xiedong@mail.ustc.edu.cn

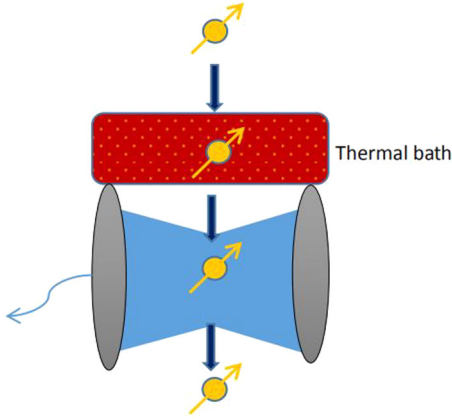


FIG. 1. Schematic diagram of the proposed quantum thermometry sequence. The TLSs pass through the thermal bath with the temperature T to be tested. Then the TLSs traverse a cavity with the decay rate κ . There is an additional thermal bath with temperature T_c in the cavity. By measuring the steady state of the cavity, the temperature T of the thermal bath can be obtained.

extra thermal bath to improve the estimation precision of the temperature.

This article is organized as follows: In Sec. II, we introduce the physical model of quantum thermometry and the corresponding master equation. In Sec. III, we utilize the partly thermalized TLS with initial coherence to obtain the Heisenberg scaling. In Sec. IV, maximal Quantum Fisher information is obtained to show whether direct photon detection and homodyne detection are the optimal measurement. We make a brief conclusion in Sec. IV.

II. QUANTUM THERMOMETRY MODEL

We consider a quantum thermometry model as shown in Fig. 1. A stream of two-level systems (TLSs) passes through the thermal bath with the temperature T to be tested. Each TLS is coupled to the thermal bath for same time duration τ_1 . During this time, information about the temperature T is encoded into the TLSs. We then consider using a cavity-QED setup to estimate the value of the temperature T . After passing through the thermal bath, the TLSs pass through a single-mode cavity one by one [23,26,27]. The interaction time between each system and the cavity model is assumed to be τ_2 .

The Hamiltonian of a single TLS is given by $H_s = \frac{\omega}{2}\sigma_z$, where ω denotes the energy separation and Pauli operator $\sigma_z = |e\rangle\langle e| - |g\rangle\langle g|$, where $|e\rangle$ is the excited state and $|g\rangle$ the ground state. We assume that the strength of coupling between TLS and the thermal bath is weak. The Born, Markov, and rotating-wave approximations can then be applied. The master equation describing the interaction can be written as [28] ($\hbar = 1, \kappa_B = 1$ throughout this article)

$$\begin{aligned} \dot{\rho}_s(t) = & -i[H_s, \rho(t)] + \gamma(1 - e^{-\omega/T})^{-1} \mathcal{D}[\sigma^-] \rho(t) \\ & + \gamma(e^{\omega/T} - 1)^{-1} \mathcal{D}[\sigma^+] \rho(t), \end{aligned} \quad (1)$$

where $\mathcal{D}[\sigma]\rho = \sigma\rho\sigma^\dagger - \frac{1}{2}(\sigma^\dagger\sigma\rho + \rho\sigma\sigma^\dagger)$, $\sigma^- = |g\rangle\langle e|$, $\sigma^+ = |e\rangle\langle g|$, and γ is a temperature-independent coupling

constant. All TLSs are initially prepared in the same state (written in the basis $\{|e\rangle, |g\rangle\}$)

$$\rho_s(t=0) = \begin{pmatrix} p_e & \lambda \\ \lambda^* & p_g \end{pmatrix},$$

where $|\lambda|^2 \leq p_e p_g$, λ is the coherence of a single TLS, and all TLSs have the same value of λ . By computing Eq. (1) analytically, we can get the density matrix of a TLS after passing through the thermal bath

$$\rho_s(t=\tau_1) = \begin{pmatrix} (p_e - \frac{\Gamma}{\Gamma+1})\xi^2 + \frac{\Gamma}{\Gamma+1} & \lambda_\tau \\ \lambda_\tau^* & (\frac{\Gamma}{\Gamma+1} - p_e)\xi^2 + \frac{1}{\Gamma+1} \end{pmatrix},$$

where $\Gamma = e^{-\omega/T}$, $\xi = \exp[-\frac{1}{2}\gamma\tau_1(\frac{1+\Gamma}{1-\Gamma})]$, and $\lambda_\tau = \lambda\xi e^{-i\omega\tau_1}$. Hence, the information of temperature T has been encoded into the TLSs.

Then, the TLSs traverse the cavity one at a time. The atomic injection rate is denoted r , which represents the average number of TLSs injected into the cavity per unit time. Simply, we consider that TLSs are resonant with the cavity mode; that is, the frequency cavity field is equal to ω . The Jaynes-Cummings Hamiltonian can describe the interaction between a single TLS and the cavity mode:

$$H = \frac{\omega}{2}\sigma_z + \omega a^\dagger a + g(a\sigma^+ + \sigma^- a^\dagger), \quad (2)$$

where a (a^\dagger) denotes the annihilation (creation) operators of the cavity field and the bosonic commutation relation $[a, a^\dagger] = 1$. We consider that the cavity also suffers from a Markovian environment with temperature T_c , the decay of the cavity can be described by [28]

$$\mathcal{L}\rho_c = \kappa(\bar{n}_{th} + 1)\mathcal{D}[a]\rho_c + \kappa\bar{n}_{th}\mathcal{D}[a^\dagger]\rho_c, \quad (3)$$

where κ is the decay rate of the cavity field and \bar{n}_{th} is the thermal average photon number, which is described by

$$\bar{n}_{th} = \frac{1}{e^{\omega/T_c} - 1}, \quad (4)$$

where T_c denotes the temperature of the extra thermal bath in the cavity.

By tracing over the degrees of freedom of the TLS, in the interaction representation, the master equation of the single-mode cavity field can be obtained in the short-interaction-time τ_2 limit ($g\tau_2 \ll 1$ and $r\tau_2 \ll 1$) [23,26,27,29–32]:

$$\dot{\rho}_c(t) \approx i[\rho_c(t), \beta a^\dagger + \beta^* a] + \gamma_1 \mathcal{D}[a]\rho_c(t) + \gamma_2 \mathcal{D}[a^\dagger]\rho_c(t), \quad (5)$$

where $\beta = \lambda_\tau r g \tau_2$, the decay rate $\gamma_1 = r(g\tau_2)^2[(p_e - \frac{\Gamma}{\Gamma+1})\xi^2 + \frac{\Gamma}{\Gamma+1}] + \kappa\bar{n}_{th}$, and the excitation rate $\gamma_2 = r(g\tau_2)^2[(\frac{\Gamma}{\Gamma+1} - p_e)\xi^2 + \frac{1}{\Gamma+1}] + \kappa(\bar{n}_{th} + 1)$. The free evolution of cavity mode has been included in Eq. (5).

III. PARTLY THERMALIZED TWO-LEVEL SYSTEMS FOR OBTAINING HEISENBERG SCALING

The steady state of the single-mode cavity carries information about the temperature T . Hence, measuring the steady cavity field can be used to estimate the value of T .

From Eq. (5), we can obtain the equation of motion of the average value of the annihilation operator,

$$\frac{d}{dt}\langle a(t) \rangle = -\frac{1}{2}(\gamma_2 - \gamma_1)\langle a(t) \rangle - i\beta, \quad (6)$$

where $\langle a(t) \rangle = \text{Tr}[\rho(t)a]$.

We can derive that

$$\langle a(t) \rangle = e^{-\frac{1}{2}(\gamma_2 - \gamma_1)t} \left[\langle a(t=0) \rangle + \frac{2i\beta}{\gamma_2 - \gamma_1} \right] - \frac{2i\beta}{\gamma_2 - \gamma_1}. \quad (7)$$

We can see that the characteristic time to reach the steady state should be $\frac{1}{\gamma_2 - \gamma_1}$. The effective TLS number which can interact with the photon during the characteristic time can be defined as

$$N_c = \frac{r}{\gamma_2 - \gamma_1}. \quad (8)$$

In the short-time τ_2 limit, we consider the parameter regime of

$$r(g\tau_2)^2 \ll \kappa. \quad (9)$$

Then, the effective TLS number can be defined as

$$N_c \approx \frac{r}{\kappa}. \quad (10)$$

To estimate the temperature, the expectations of $\{(a^\dagger a)^2, a^{\dagger 2}, a^2, a^\dagger a, a, a^\dagger\}$ need to be derived. From Eq. (5), we can obtain the complete dynamical equations of $\{((a^\dagger a)^2), (a^\dagger a a^\dagger), (a^\dagger a), (a^{\dagger 2}), (a^2), (a^\dagger a), (a), (a^\dagger)\}$. Then, the expectations values for the steady state can be obtained [26]:

$$\langle a \rangle = \langle a^\dagger \rangle^* = \frac{2i\beta}{\gamma_1 - \gamma_2}, \quad (11)$$

$$\langle a^2 \rangle = \langle a^{\dagger 2} \rangle^* = \frac{-4\beta^2}{(\gamma_1 - \gamma_2)^2}, \quad (12)$$

$$\langle a^\dagger a \rangle = \frac{\gamma_1}{\gamma_2 - \gamma_1} + \frac{4|\beta|^2}{(\gamma_2 - \gamma_1)^2}, \quad (13)$$

$$\langle (a^\dagger a)^2 \rangle = \frac{\gamma_1(\gamma_1 + \gamma_2)}{(\gamma_1 - \gamma_2)^2} - \frac{(12\gamma_1 + 4\gamma_2)|\beta|^2}{(\gamma_1 - \gamma_2)^3} + \frac{16|\beta|^4}{(\gamma_2 - \gamma_1)^4}. \quad (14)$$

From the above equations, we can see that direct photon detection (with the measurement operator $a^\dagger a$) can be used to estimate the value of the temperature T of the sample to be tested. According to the error propagation formula, the uncertainty of T can be derived as

$$\delta^2 T = \frac{\langle (a^\dagger a)^2 \rangle - \langle (a^\dagger a) \rangle^2}{(\partial \langle a^\dagger a \rangle / \partial T)^2}. \quad (15)$$

First, we consider that there is no extra thermal fluctuations around the cavity; that is, $\bar{n}_{th} = 0$ ($T_c = 0$). When the TLS is initially prepared with no coherence ($\lambda = 0$), the standard quantum limit $\delta^2 T \sim 1/N_c$ can be obtained. For obtaining the Heisenberg scaling, the following prerequisites must be met:

$$4N_c |\lambda \xi|^2 \gg \left(p_e - \frac{\Gamma}{\Gamma + 1} \right) \xi^2 + \frac{\Gamma}{\Gamma + 1}. \quad (16)$$

It means that the initial coherence ($\lambda \neq 0$) is necessary. Besides, the TLSs cannot be fully thermalized; that is, $\xi \neq 0$.

Namely, the thermalization time τ_1 is short. The optimal thermalization time can be derived as

$$\tau_{1\text{opt}} \approx \frac{2(1 - \Gamma)}{\gamma(1 + \Gamma)}. \quad (17)$$

The corresponding optimal estimation precision with the direct detection can be read as

$$\delta^2 T_{\text{opt}} \approx \frac{e^2 T^4}{(4N_c g \tau_2 \omega \lambda)^2 \text{csch}^2 \frac{\omega}{T}}. \quad (18)$$

It shows that the Heisenberg scaling is achieved, $\delta^2 T \sim 1/(N_c)^2$. Initial coherence and partly thermalization can help to improve the estimation precision of temperature in the cavity set-up. This is attributed to the fact that the initial coherence induces entanglement between TLSs by interacting with the common cavity. Comparing with the full thermalization, partial thermalization can encode the information of temperature into TLSs without completely destroying the initial coherence.

Then, we consider that there is an extra thermal bath in the cavity (ETBC); that is, $T_c \neq 0$. Let us think about two different cases: One case is that ETBC is independent with the thermal bath to be tested; that is, T_c and T are independent parameters. For $T_c \rightarrow \infty$, the optimal thermalization time

$$\tau_{1\text{opt}} \approx \frac{(1 - \Gamma)}{\gamma(1 + \Gamma)}. \quad (19)$$

This means the optimal thermalization time $\frac{(1-\Gamma)}{\gamma(1+\Gamma)} < \tau_{1\text{opt}} < \frac{2(1-\Gamma)}{\gamma(1+\Gamma)}$ for general values of T_c . For the sake of discussion, in what follows we still use the value of τ_1 given by Eq. (17). By direct photon detection, under the condition in Eq. (16) and the interaction time given by Eq. (17), the estimation precision of T is expressed as

$$\delta^2 T_{\text{ind}} \approx \frac{e^2 T^4 (1 + 2\bar{n}_{th})}{(4N_c g \tau_2 \omega \lambda)^2 \text{csch}^2 \frac{\omega}{T}} + \frac{e^4 T^4 (1 + \bar{n}_{th}) \bar{n}_{th}}{64(N_c g \tau_2 \lambda)^4 \omega^2 \text{csch}^2 \frac{\omega}{T}}, \quad (20)$$

where $\bar{n}_{th} = \frac{1}{e^{\omega/T_c} - 1}$.

In the other case, ETBC also has the information of the temperature T to be tested in the thermal bath. We assume that they have the same temperature ($T_c = T$). For example, ETBC and the thermal bath are in thermal equilibrium with each other. The corresponding estimation precision of T is expressed as

$$\delta^2 T_{\text{equ}} \approx \frac{T^4 [(1 + 2\bar{n}'_{th})(2eN_c g \tau_2 \lambda)^2 + (1 + \bar{n}'_{th})\bar{n}'_{th} e^4]}{\omega^2 \left[8 \text{csch} \frac{\omega}{T} (N_c g \tau_2 \lambda)^2 - \frac{e^2 \Gamma}{(\Gamma - 1)^2} \right]^2}, \quad (21)$$

where $\bar{n}'_{th} = \frac{1}{e^{\omega/T} - 1}$. From Eqs. (20) and (21), we find that $\delta^2 T_{\text{ind}}$ is less than $\delta^2 T_{\text{equ}}|_{T \rightarrow T_c}$, as shown in Fig. 2. This shows that direct photon detection does not obtain more information about the temperature T when ETBC also carries the information of temperature T . In contrast, the information from ETBC destroys the ability of direct photon detection to access the information of T .

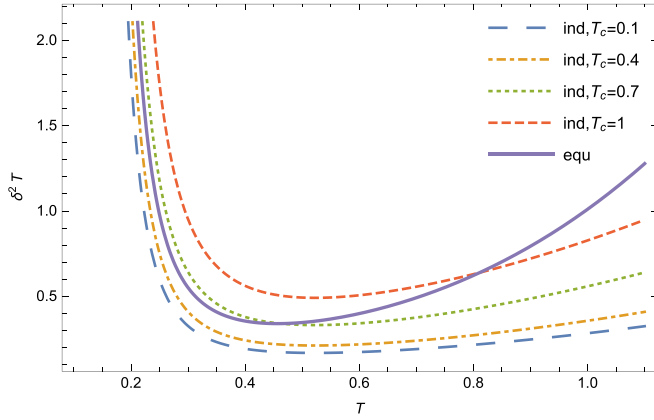


FIG. 2. Diagram of estimation temperature T with direct photon detection. In this diagram, “ind” denotes the case where ETBC is independent of the thermal bath and “equ” denotes the case where ETBC is thermalized with the thermal bath. In the case of “ind,” the high temperature of ETBC will reduce the measurement precision of T . For the same value of ETBC, the uncertainty of T in the case of “equ” is larger than that in the case of “ind.” Here, the parameters are given by $\omega = 1$, $g\tau_2 = 0.3$, $N_c = 10$, $\lambda = 0.5$, in arbitrary units.

IV. MAXIMAL QUANTUM FISHER INFORMATION

Due to that the effective Hamiltonian in Eq. (5) is a quadratic form, the final steady state will be a Gaussian state. Then the quantum Fisher information (QFI) about the temperature T can be calculated by [33]

$$\mathcal{F} = \text{Tr}(G_T \partial_T C) + (\partial_T \langle \vec{R} \rangle)^T C^{-1} \partial_T \langle \vec{R} \rangle, \quad (22)$$

where the first moment is expressed as $\vec{R} = (\frac{a+a^\dagger}{\sqrt{2}}, \frac{a-a^\dagger}{i\sqrt{2}})$ and the entries of the covariance matrix C is expressed as $C_{ij} = \frac{1}{2} \langle R_i R_j + R_j R_i \rangle - \langle R_i \rangle \langle R_j \rangle$. For a single-mode Gaussian state, G_T is written as

$$G_T = \frac{4c^2 - 1}{4c^2 + 1} \Omega (\partial_T J) \Omega, \quad (23)$$

where $c = \sqrt{\det C}$ is the symplectic eigenvalue of C , $J = \frac{1}{4c^2 + 1} C$, and Ω is the symplectic matrix defined as $i\sigma_y$.

With the above equations, the QFI can be obtained. When the temperature of ETBC is independent of the temperature of the thermal bath, for the interaction time given by Eq. (17), the maximal QFI is

$$\mathcal{F}_{\text{ind}} = \frac{(4N_c g\tau_2 \omega \lambda)^2 \text{csch}^2 \frac{\omega}{T}}{e^2 T^4 (1 + 2\bar{n}_{th})}, \quad (24)$$

where $\bar{n}_{th} = \frac{1}{e^{\omega/T} - 1}$. When the temperature of ETBC is always equal to the temperature of the sample ($T_c = T$), the maximal QFI is

$$\mathcal{F}_{\text{equ}} = \frac{(4N_c g\tau_2 \omega \lambda)^2 \text{csch}^2 \frac{\omega}{T}}{e^2 T^4 (1 + 2\bar{n}'_{th})} + \frac{w^2 \bar{n}'_{th} (1 + \bar{n}'_{th})}{2T^4}, \quad (25)$$

where $\bar{n}'_{th} = \frac{1}{e^{\omega/T} - 1}$.

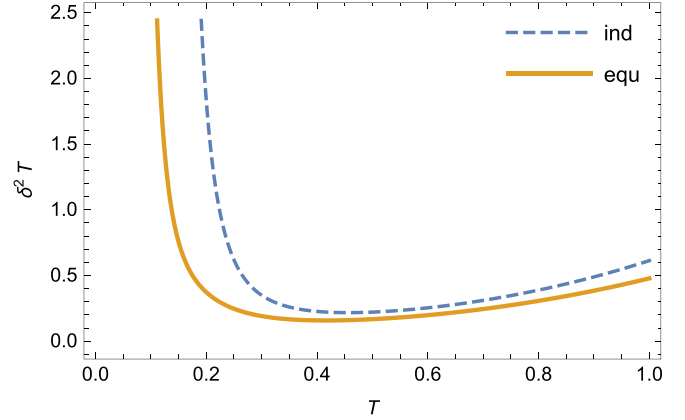


FIG. 3. Diagram of estimation temperature T with optimal detection. In this diagram, “ind” denotes the case of that ETBC is independent with the thermal bath and “equ” denotes the case where ETBC is thermalized with the thermal bath. For the same value of T_c , the uncertainty in T in the case of “equ” is less than that in the case of “ind.” Here, the parameters are given by $\omega = 1$, $g\tau_2 = 0.3$, $N_c = 10$, $\lambda = 0.5$ in arbitrary units.

According to the quantum Cramér-Rao bound [3], we can get the uncertainty of temperature T with the optimal measurement in two conditions:

$$\delta^2 T_{\text{ind}} \geq \frac{1}{\mathcal{F}_{\text{ind}}} = \frac{e^2 T^4 (1 + 2\bar{n}_{th})}{(4N_c g\tau_2 \omega \lambda)^2 \text{csch}^2 \frac{\omega}{T}}, \quad (26)$$

$$\delta^2 T_{\text{equ}} \geq \frac{1}{\mathcal{F}_{\text{equ}}} = \frac{1}{\frac{(4N_c g\tau_2 \omega \lambda)^2 \text{csch}^2 \frac{\omega}{T}}{e^2 T^4 (1 + 2\bar{n}'_{th})} + \frac{\omega^2 \bar{n}'_{th} (1 + \bar{n}'_{th})}{2T^4}}. \quad (27)$$

Comparing Eq. (26) with Eq. (27), we find that $\delta^2 T_{\text{equ}}|_{T=T_c} < \delta^2 T_{\text{ind}}|_{T=T_c}$ for $T_c \neq 0$, as shown in Fig. 3. This shows that, when ETBC also has the information of the temperature T to be tested, the optimal measurement can utilize the information from ETBC to further improve the measurement precision of T , contrary with the results from direct photon detection in the section above. This means that direct photon detection is not the optimal measurement strategy.

When there is no ETBC ($T_c = 0$), we can find that the estimation uncertainty in Eq. (26) is equal to the result in Eq. (18). It shows that direct photon detection is the optimal measurement for the case of $T_c = 0$. When $T_c \neq 0$, direct photon detection is not optimal by comparing Eqs. (20), (21), (26), and (27).

By a rigorous derivation, we achieved that the balanced homodyne detection [34] with the quadrature operator $\frac{a-a^\dagger}{i\sqrt{2}}$ is the optimal measurement in the case where ETBC is independent of the thermal bath. With the optimal thermalization time given by Eq. (17), the estimation precision of T can be obtained with the homodyne detection

$$\delta^2 T_{\text{ind}} = \frac{e^2 T^4 (1 + 2\bar{n}_{th})}{(4N_c g\tau_2 \omega \lambda)^2 \text{csch}^2 \frac{\omega}{T}}, \quad (28)$$

$$\delta^2 T_{\text{equ}} = \frac{e^2 T^4 (1 + 2\bar{n}'_{th})}{(4N_c g\tau_2 \omega \lambda)^2 \text{csch}^2 \frac{\omega}{T}}. \quad (29)$$

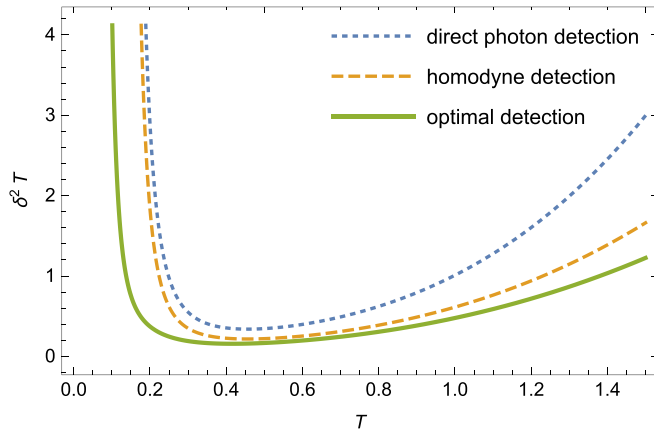


FIG. 4. Diagram of estimation temperature T with three ways of measurements in the case where ETBC is in thermal equilibrium with the thermal sample. This figure shows that homodyne detection performs better than direct detection. However, homodyne detection does not perform as well as the optimal measurement. Here, the parameters are the same as in the previous figures.

From Eqs. (20), (26), and (28), we can see that, for $T_c = 0$ ($\bar{n}_{th} = 0$), homodyne detection and direct detection are both optimal measurements; for $T_c \neq 0$ homodyne detection is the optimal measurement, which performs better than direct photon detection.

However, if ETBC is in thermal equilibrium with the thermal sample (see Fig. 4), homodyne detection either is not the optimal measurement. In this case, we find that the symmetric logarithmic derivative (SLD) for the temperature T depends on T itself. Adaptive measurement is needed to obtain the optimal estimation precision of T . Finding a realizable and simple optimal measurement is definitely worth further investigation.

V. CONCLUSION

We have used a cavity-QED setup to measure the temperature of a thermal bath. Our result shows that the Heisenberg scaling for estimating the nonunitary parameter T can be achieved. The two-level systems pass through the thermal bath, then carry the information of the temperature of the thermal bath. Following that, the encoded two-level systems are injected into a single-mode cavity one by one. By measuring the steady-state of the cavity, information of the temperature

can be obtained. Preparing the atomic entanglement before they interact with the cavity field is unnecessary for measuring the temperature in our scheme. The initial coherence of the two-level systems induce the effective coherent driving to the cavity field, leading to obtain the Heisenberg scaling. The need for the two-level systems are not thermalized fully by the thermal bath. The optimal interaction time between each two-level system and the thermal bath has been derived. By calculating the maximal quantum Fisher information, we find that direct photon detection and homodyne detection are both optimal measurements when there is no extra thermal bath in the cavity ($T_c = 0$). When there is an extra thermal bath in the cavity independent of the thermal bath to be tested, homodyne detection is the optimal measurement. Moreover, direct photon detection obtains less information of the temperature in the case where the extra thermal bath in the cavity is in thermal equilibrium with the thermal bath. This means that more ways of encoding information of the temperature destroy the ability to access information for direct photon detection. The optimal measurement shows that more ways of encoding information can improve the estimation precision.

Our scheme is feasible, which should be realized in recent experiments with a nanohole-array aperture [23], the Rydberg atom plus microwave cavity system [35], and a superconducting circuit QED system of a transmission line resonator coupled with a charge qubit [36,37]. In superconducting circuit QED system, the coupling between the transmission line resonator and the charge qubit can be switched on or off by tuning the magnetic flux [38]. For instance, taking the following parameters: the resonator frequency $\omega = 2\pi \times 20$ GHz, the coupling strength $g = 2\pi \times 290$ kHz, the cavity decay rate $\kappa = 2\pi \times 75$ kHz, the atomic injection rate $r = 2\pi \times 2$ MHz, the interaction time $(\tau_1, \tau_2) \sim (10^3, 10)$ ns, the temperature $T = 200$ mK, and $p_e = \lambda = 1/2$, simple calculations show that the restricted conditions in Eqs. (9) and (16) can be satisfied. It will promote the development of the quantum thermometry and measurement methods based on the QED setup.

ACKNOWLEDGMENTS

We acknowledge Q. He and M. Fadel for helpful discussion and constructive comments on the paper. This research was supported by the National Natural Science Foundation of China under Grant No. 11747008 and the Natural Science Foundation of Guangxi Province under Grant No. 2016GXNSFBA380227.

-
- [1] V. Giovannetti, S. Lloyd, and L. Maccone, *Science* **306**, 1330 (2004).
 - [2] V. Giovannetti, S. Lloyd, and L. Maccone, *Phys. Rev. Lett.* **96**, 010401 (2006).
 - [3] K. Bongs, R. Launay, and M. A. Kasevich, *Appl. Phys. B: Lasers Opt.* **84**, 599 (2006).
 - [4] M. G. A. Paris, *Int. J. Quantum Inform.* **7**, 125 (2009).
 - [5] M. A. Taylor, J. Janousek, V. Daria, J. Knittel, B. Hage, H.-A. Bachor, and W. P. Bowen, *Nat. Photonics* **7**, 229 (2013).
 - [6] S. Slussarenko, M. M. Weston, H. M. Chrzanowski, L. K. Shalm, V. B. Verma, S. W. Nam, and G. J. Pryde, *Nat. Photonics* **11**, 700 (2017).
 - [7] D. Xie, C. Xu, and A. Wang, *Quantum Inf. Process.* **16**, 155 (2017).
 - [8] J. Yang, C. Elouard, J. Splettstoesser, B. Sothmann, R. Sánchez, and A. N. Jordan, *Phys. Rev. B* **100**, 045418 (2019).
 - [9] P. P. Hofer, J. B. Brask, M. Perarnau-Llobet, and N. Brunner, *Phys. Rev. Lett.* **119**, 090603 (2017).

- [10] M. Mehboudi, A. Sanpera, and L. A. Correa, *J. Phys. A: Math. Theor.* **52**, 303001 (2019).
- [11] L. Spietz, K. W. Lehnert, I. Siddiqi, and R. J. Schoelkopf, *Science* **300**, 1929 (2003).
- [12] L. Spietz, R. J. Schoelkopf, and P. Pari, *Appl. Phys. Lett.* **89**, 183123 (2006).
- [13] S. Gasparinetti, F. Deon, G. Biasiol, L. Sorba, F. Beltram, and F. Giazotto, *Phys. Rev. B* **83**, 201306(R) (2011).
- [14] M. Xiao, L. A. Wu, and H. J. Kimble, *Phys. Rev. Lett.* **59**, 278 (1987).
- [15] P. Grangier, R. E. Slusher, B. Yurke, and A. LaPorta, *Phys. Rev. Lett.* **59**, 2153 (1987).
- [16] I. Kruse, K. Lange, J. Peise, B. Lücke, L. Pezzé, J. Arlt, W. Ertmer, C. Lisdat, L. Santos, A. Smerzi, and C. Klempt, *Phys. Rev. Lett.* **117**, 143004 (2016).
- [17] R. Schnabel, N. Mavalvala, D. E. McClelland, and P. K. Lam, *Nat. Commun.* **1**, 121 (2010).
- [18] J. Aasi *et al.*, *Nat. Photonics* **7**, 613 (2013).
- [19] P. Cappelaro, J. Emerson, N. Boulant, C. Ramanathan, S. Lloyd, and D. G. Cory, *Phys. Rev. Lett.* **94**, 020502 (2005).
- [20] T. Nagata, R. Okamoto, J. L. O'Brien, K. Sasaki, and S. Takeuchi, *Science* **316**, 726 (2007).
- [21] L. A. Correa, M. Mehboudi, G. Adesso, and A. Sanpera, *Phys. Rev. Lett.* **114**, 220405 (2015).
- [22] T. M. Stace, *Phys. Rev. A* **82**, 011611(R) (2010).
- [23] J. Kim, D. Yang, S. Oh, and K. An, *Science* **359**, 662 (2018).
- [24] V. Paulisch, M. Perarnau-Llobet, A. González-Tudela, and J. I. Cirac, *Phys. Rev. A* **99**, 043807 (2019).
- [25] D. W. Wang and M. O. Scully, *Phys. Rev. Lett.* **113**, 083601 (2014).
- [26] W. Cheng, S. C. Hou, Zhihai Wang, and X. X. Yi, *Phys. Rev. A* **100**, 053825 (2019).
- [27] D. Vitali and P. Tombesi, *Phys. Rev. A* **65**, 012305 (2001).
- [28] M. O. Scully and M. S. Zubairy, *Quantum Optics* (Cambridge University Press, Cambridge, 1997).
- [29] M. Orszag, *Quantum Optics: Including Noise Reduction, Trapped Ions, Quantum Trajectories, and Decoherence* (Springer, Berlin, 2000).
- [30] J. D. Cresser, *Phys. Rev. A* **46**, 5913 (1992); J. D. Cresser and S. M. Pickles, *Quantum Semiclass. Opt.* **8**, 73 (1996).
- [31] D. Meschede, H. Walther, and G. Müller, *Phys. Rev. Lett.* **54**, 551 (1985).
- [32] J. Bergou, L. Davidovich, M. Orszag, C. Benkert, M. Hillery, and M. O. Scully, *Phys. Rev. A* **40**, 5073 (1989).
- [33] A. Monras, [arXiv:1303.3682](https://arxiv.org/abs/1303.3682).
- [34] H. Wiseman and G. Milburn, *Quantum Measurement and Control* (Cambridge University Press, New York, 2010).
- [35] M. Brune, F. Schmidt-Kaler, A. Maali, J. Dreyer, E. Hagley, J. M. Raimond, and S. Haroche, *Phys. Rev. Lett.* **76**, 1800 (1996).
- [36] A. Blais, R. S. Huang, A. Wallraff, S. M. Girvin, and R. J. Schoelkopf, *Phys. Rev. A* **69**, 062320 (2004).
- [37] A. Wallraff, D. I. Schuster, A. Blais, L. Frunzio, R. S. Huang, J. Majer, S. Kumar, S. M. Girvin, and R. J. Schoelkopf, *Nature (London)* **431**, 162 (2004).
- [38] M. Hofheinz, H. Wang, M. Ansmann, R. C. Bialczak, E. Lucero, M. Neeley, A. D. O'Connell, D. Sank, J. Wenner, J. M. Martinis, and A. N. Cleland, *Nature (London)* **459**, 546 (2009).